Paleoceanography and Paleoclimatology

RESEARCH ARTICLE
10.1029/2018PA003477

Deglacial Thinning of the Laurentide Ice Sheet in the Adirondack Mountains, New York, USA, Revealed by ^{36}Cl Exposure Dating

Aaron M. Barth[1], Shaun A. Marcott[1], Joseph M. Licciardi[2], and Jeremy D. Shakun[3]

[1]Department of Geoscience, University of Wisconsin-Madison, Madison, WI, USA, [2]Department of Earth Sciences, University of New Hampshire, Durham, NH, USA, [3]Department of Earth and Environmental Sciences, Boston College, Chestnut Hill, MA, USA

Key Points:
- The ^{36}Cl exposure ages from the Adirondacks show regional ice sheet thinning histories
- The Laurentide Ice Sheet experienced two-phase thinning in this region ~21–14 ka
- Gradual thinning was followed by rapid retreat coincident with the Bølling-Allerød

Supporting Information:
- Supporting Information S1
- Table S1

Correspondence to:
A. M. Barth,
abarth@ehc.edu

Citation:
Barth, A. M., Marcott, S. A., Licciardi, J. M., & Shakun, J. D. (2019). Deglacial thinning of the Laurentide Ice Sheet in the Adirondack Mountains, New York, USA, revealed by ^{36}Cl exposure dating. *Paleoceanography and Paleoclimatology*, *34*. https://doi.org/10.1029/2018PA003477

Received 21 SEP 2018
Accepted 2 MAY 2019
Accepted article online 8 MAY 2019

Abstract Future changes in sea level will largely be dictated by changes in the world's ice sheets. Yet the magnitude and rate at which these ice sheets will respond to climate change remain uncertain, necessitating a deeper investigation into past ice sheet-climate interactions. Numerous studies have documented the timing and pattern of Laurentide Ice Sheet margin retreat since the Last Glacial Maximum, but few studies have provided vertical constraints necessary for accurate sea level contribution estimates. Here we present 21 ^{36}Cl ages from boulder and bedrock samples along vertical transects spanning ~1,000 m of relief from multiple peaks in the Adirondack Mountains of northeastern New York, USA. Our exposure ages span the Last Glacial Maximum through the last deglaciation, with the highest-elevation sites (~1,500 m) ranging between 25 and 19 ka, and the lower elevation sites (≤1,300 m) between 16 and 13 ka. These data suggest gradual ice sheet thinning of 200 m initiated at ~20 ka followed by more rapid surface lowering of 1,000 m approximately coincident with Bølling-Allerød warming.

1. Introduction

Accurate reconstructions of both the extent and height of former ice sheets are important for understanding how they responded to and impacted regional-to-global climate (Braconnot et al., 2012; Hostetler et al., 2000), ocean circulation (Zhang et al., 2014), and sea level (Lambeck et al., 2014; Peltier et al., 2015). During the Last Glacial Maximum (LGM; 26–19 ka; Clark et al., 2009), the Laurentide Ice Sheet (LIS) covered much of northern North America and held the equivalent of 76–85 m of eustatic sea level (Clark et al., 2009; Clark & Mix, 2002). The retreat history of the LIS margin is well constrained following the LGM (Dyke, 2004), but changes in ice thickness are still poorly known due to a scarcity of geochronologic controls on ice sheet surface elevation changes. Such constraints are valuable because they provide geologic limits on ice-volume estimates useful for modeling future sea level changes (Liu et al., 2016).

The chronology of LIS margin retreat in New England has been defined by multiple dating methods, including minimum-limiting basal radiocarbon ages from ponds and lakes (Dyke, 2004), lake varve chronologies (Ridge et al., 2012; Thompson et al., 2017), and in situ terrestrial cosmogenic nuclide surface exposure dating of terminal and recessional moraines (Balco & Schaefer, 2006; Bromley et al., 2015; Corbett et al., 2017). A few additional studies have begun to place vertical limits on the southeastern LIS based on surface exposure ages from high mountain summits (>1,300 m above sea level (asl)) in Maine and New Hampshire (Bierman et al., 2015; Davis et al., 2015), a vertical transect in Vermont (Corbett et al., 2019), and low-elevation peaks (<400 m) in coastal Maine (Koester et al., 2017). Yet these direct age constraints on LIS thinning are sparse, and data further inland from the Atlantic coast are necessary to provide additional insight on the deglacial surface lowering of the interior of the LIS.

In this study, we expand the existing data coverage westward by reconstructing ice sheet thinning between 400 and 1,560 m asl in the Adirondack Mountains of upstate New York using 21 new ^{36}Cl surface exposure ages (Figure 1). We place this reconstruction within the context of the regional glacial history from prior studies, and consider its relationship to meltwater routing pathways. These new data provide a record of high-elevation vertical thinning of the LIS in the interior northeast United States as the ice sheet retreated from its LGM position through the deglacial period spanning several well-documented hemispheric-scale climate (e.g., Bølling-Allerød) and eustatic sea level changes (e.g., Meltwater Pulse 1a).

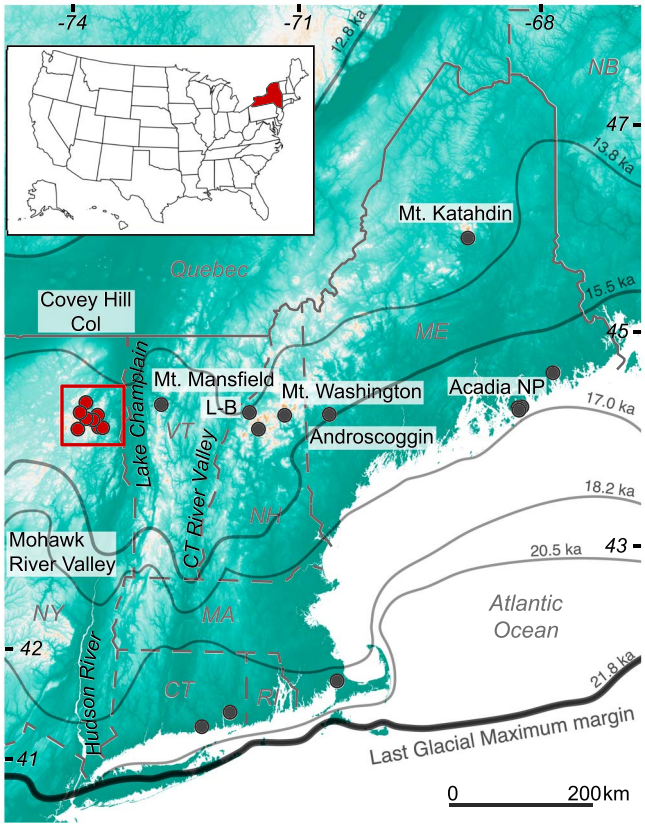

Figure 1. Regional map of the northeast United States. Surface exposure dating locations from this study denoted with red circles and from other studies (Balco & Schaefer, 2006; Bierman et al., 2015; Bromley et al., 2015; Koester et al., 2017) denoted with gray circles. Contour lines represent the Last Glacial Maximum to late deglacial margin of the Laurentide Ice Sheet (Dyke, 2004). Box indicates the study location. Littleton-Bethlehem (L-B) moraines labeled. Inset map shows the location of New York within the United States.

2. Geologic Setting

The Adirondack Mountains are part of a large, domelike intrusive structure in northern New York State that is composed of high-grade metamorphic rocks of the Grenville Structural Province (Isachsen & Fisher, 1970; Kemp, 1920). The St. Lawrence River and Lake Champlain Valleys to the north and east acted as conduits for ice flow during the last glacial period. To the south, the Mohawk River Valley features strath terraces recording periods of meltwater drainage to the Hudson River during the last deglaciation (Porreca et al., 2018). Numerous high-elevation peaks composed primarily of anorthosite make up the interior of the mountain range (Ashwal, 1993) and reach up to 1,600 m asl, while valley floor elevations between the peaks drop to 400–500 m asl. During the last ice age, the Adirondack Mountains were completely overtopped by the LIS (Kemp, 1898), as evidenced by erratic boulders and cobbles on and glacial smoothing of the high peaks. Glacial striations on bedrock outcrops are predominantly oriented in a north-south direction (Ogilvie, 1902). Coarse gravel to sandy till covers much of the valley floors (Denny, 1974) and moraines within the Adirondacks are subdued compared to the expansive terminal moraines of the LIS ~400 km to the south, which suggests the persistence of active ice as the ice sheet retreated through the region ~13 ka (Dyke, 2004; Figure 1).

3. Material and Methods

This study uses ^{36}Cl surface exposure dating to constrain the timing of ice sheet thinning in the Adirondacks as the LIS retreated from the mountain peaks during the last deglacial period. As part of this study, we sampled glacially deposited boulders (n = 17) and ice-scoured bedrock (n = 4) on multiple peaks in an ~800-km^2 region of the Adirondack Mountains for ^{36}Cl surface exposure dating (Figure 1). All samples are composed of locally sourced, pyroxene-rich anorthosite (Denny, 1974) and were collected using hammer and chisels from local high points and bedrock benches (Figure 2). Selected boulders were >1 m in height flat-topped, and showed minimal signs of erosion or pitting. Boulder and bedrock samples were collected from surfaces that exhibited glacial sculpting and abrasion, respectively. Most boulders rested directly on exposed bedrock and are therefore less likely to have been exhumed from till cover. Surface inclination was measured using a Brunton compass. Latitude, longitude, and altitude for each sample were recorded using a handheld GPS. Topographic shielding was determined in the field with an inclinometer and calculated using the CRONUS Topographic Shielding calculator (Balco et al., 2008).

Samples were processed for chlorine extraction at the University of New Hampshire cosmogenic nuclide laboratory using the methods of Stone et al. (1996) as modified by Licciardi et al. (2008). The upper 2 cm of whole rock samples was crushed to a 125–250-μm size fraction, wet sieved, and ultrasonically cleaned with deionized water. Crushed samples were pretreated with 2% HNO_3 and spiked with the University of New Hampshire ^{37}Cl carrier, which has an enrichment of 98.21%. Sample dissolution was carried out with a HF–HNO_3 solution. Removal of insoluble fluorides was done through centrifugation. The addition of $AgNO_3$ precipitated Cl as AgCl, which was purified by redissolving with NH_4OH and adding $BaNO_3$ to precipitate sulfate as $BaSO_4$. The final AgCl was precipitated with the addition of 2M HNO_3 and $AgNO_3$, washed repeatedly in deionized water, and dried.

The ^{35}Cl/^{37}Cl and ^{36}Cl/^{37}Cl ratios were measured at the Center for Accelerator Mass Spectrometry at Lawrence Livermore National Laboratory. Major and trace element compositional data were measured at SGS Minerals Services in Ontario, Canada. Cl concentration was calculated from the AMS data following the isotope dilution methods of Faure (1986). Reported sample ^{36}Cl concentrations are corrected for blanks. Analytical data are provided in Data Sets S1–S3.

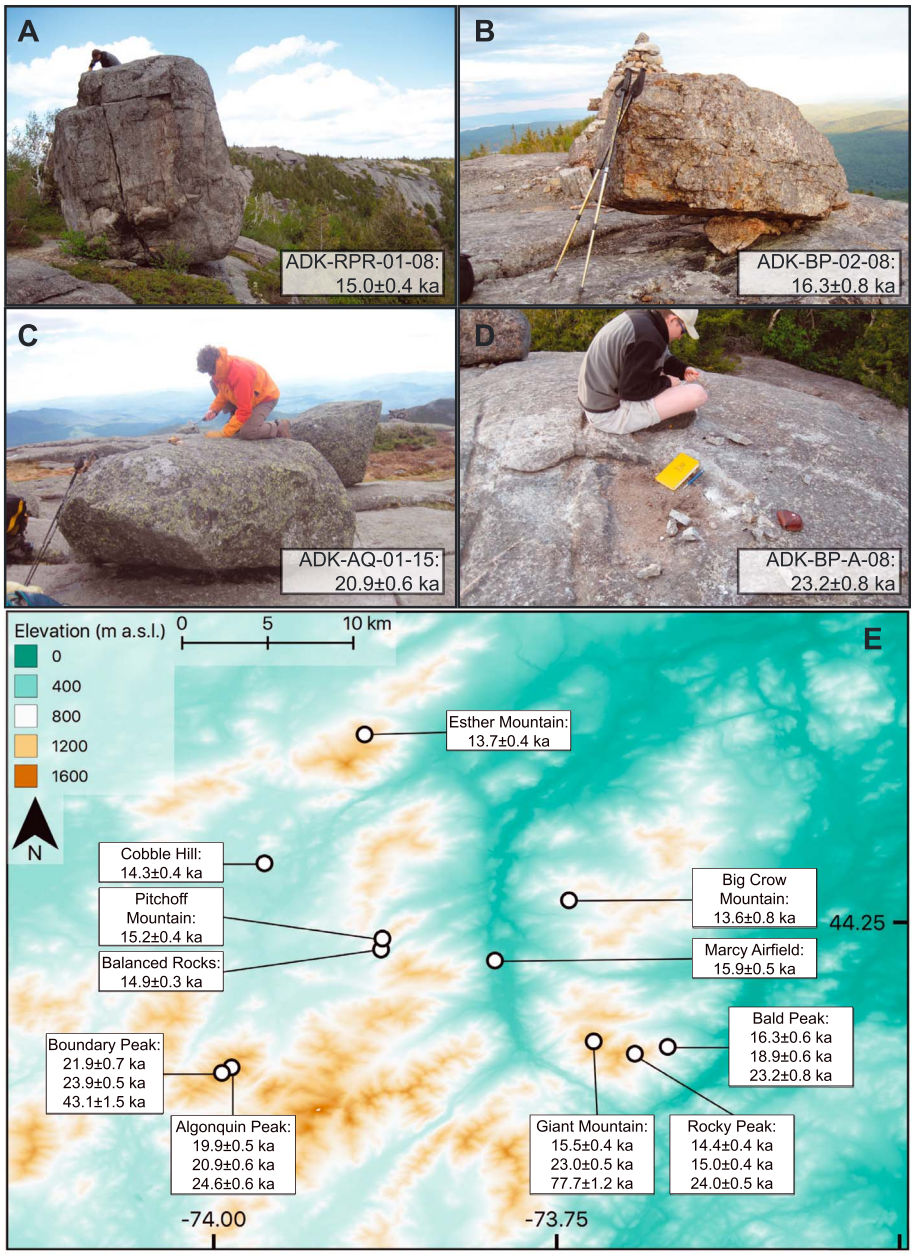

Figure 2. Boulder and bedrock samples. (a) Sampled boulders from Rocky Peak. Note the large size of the boulder and position near the cliff edge of ice-scoured bedrock with little to no soil or till cover. (b) Boulder sample from Bald Peak. (c) Boulder sample from Algonquin Peak. (d) Bedrock sample from Bald Peak. (e) Topographic map of study area and sample locations. The ^{36}Cl ages for each site are grouped in boxes and reported with 1σ uncertainty. Latitude and longitude reported as degree decimal.

Ages were calculated using CRONUScalc of Marrero et al. (2016), and the time- and nuclide-dependent "LSDn" scaling scheme (Lifton et al., 2014). Sensitivity tests for erosion were conducted though all sampled surfaces showed minimal signs of erosion (Table S1). Previously reported ^{10}Be and ^{26}Al surface exposure ages from other regional studies were recalculated with the online calculator v.3 of Balco et al. (2008), the regional northeast North America production rate (Balco et al., 2009), and LSDn scaling scheme for consistency and comparison. All ages are reported with analytic uncertainty unless otherwise noted with full production rate uncertainty reported in the Data Set S1 in the supporting information. Details of all samples, measurements, sensitivity tests, and age calculations are provided in the supporting information.

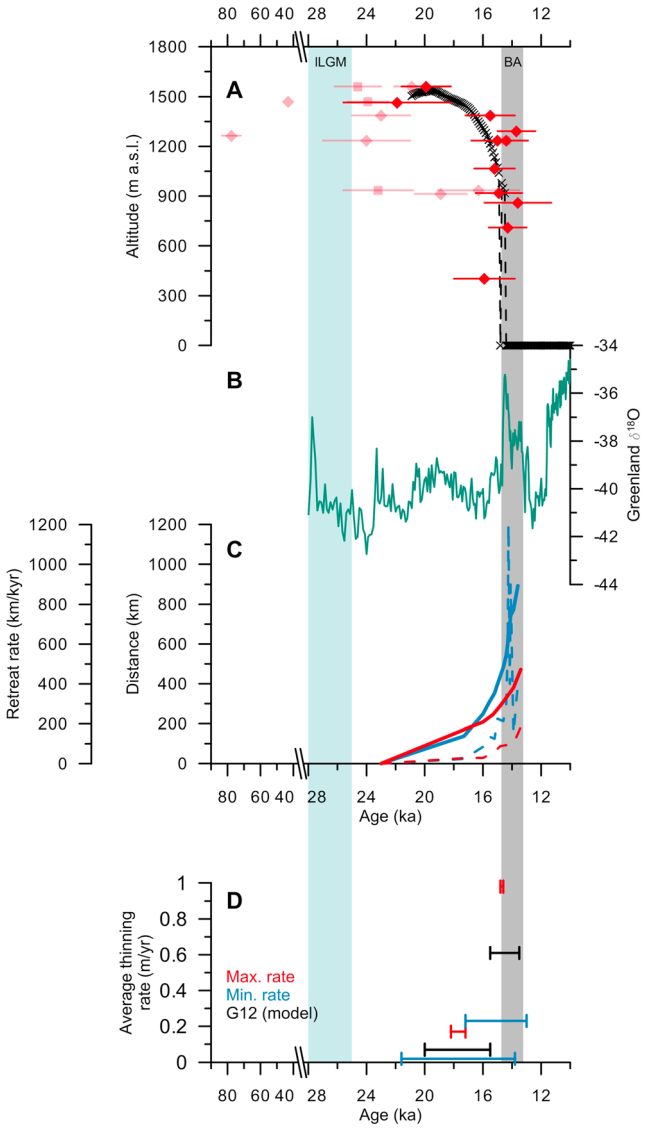

Figure 3. Surface exposure ages versus elevation and average ice sheet thinning rates. (a) Symbols indicate individual surface exposure ages with 1-sigma analytical uncertainty; diamonds are boulder samples, and squares are bedrock samples. Darker symbols indicate the youngest exposure age at any given elevation. Dashed line indicates ice sheet surface elevation in this area as determined from model output (Gregoire et al., 2012). (b) Oxygen isotope values from the GISP2 Greenland ice core (Rasmussen et al., 2008). (c) Retreat of the southeastern sector of the Laurentide Ice Sheet as determined by the North American Varve Chronology (Ridge et al., 2012). Blue line represents time-distance plot of retreat through the Connecticut River Valley; red line represents the Hudson River Valley. Dashed lines represent the retreat rate in each valley. (d) Average thinning rate of the Laurentide Ice Sheet over the Adirondacks for two intervals. Blue and red bars indicate minimum and maximum average thinning rates, respectively, as determined from the ^{36}Cl data. Black bar represents average thinning rate as determined from the model. Bar width represents the time interval over which the thinning rate is calculated. Gray bar indicates the timing of the Bolling-Allerod warm interval. Blue bar indicates the timing of the local Last Glacial Maximum (Balco et al., 2002).

4. Results

The ^{36}Cl surface exposure ages range from 24.6 ± 0.6 to 13.6 ± 0.8 ka (n = 19), excluding two outliers of 43.1 ± 1.5 and 77.7 ± 1.2 ka (Figure 2e and Data Set S1). Ages from predominantly higher elevations (>1,300 m asl) range from 24.6 ± 0.6 to 15.5 ± 0.4 ka (n = 7), whereas ages derived from lower elevations (403 to 1,292 m asl) are between 24.0 ± 0.5 and 13.6 ± 0.8 ka (n = 12). Of the higher-elevation ages, six of seven are between 24.6 ± 0.6 and 19.9 ± 0.5 ka, while at the lower elevations, nine of 12 ages are within 15.9 ± 0.5 and 13.6 ± 0.8 ka.

Scatter among ages in our data set, particularly those from closely adjacent sites, suggests the influence of geologic processes (Figures 2e and 3c). Two primary influences on the exposure age chronometer are isotope inheritance from previous exposure and postdepositional shielding (Applegate et al., 2010; Heyman et al., 2011; Putkonen & Swanson, 2003). We consider exhumation to be an unlikely source of scatter in the boulder ages since all boulders were large (>1 m) and rested on ice-scoured bedrock with little to no till (Figure 2). Indeed, nearly all bedrock ages are older than nearby boulder ages, consistent with minimal influence of exhumation. Instead, we consider prior nuclide inheritance the likely source of scatter in our data set, and suggest that it could explain the generally older ages on bedrock because glacial transport of boulders is more likely to remove surface material irradiated during previous periods of exposure. However, minimal erosion of the locally sourced boulders during glacial transport may also explain some of the age scatter. Although inheritance cannot be fully ruled out for the entirety of the boulder ages in our study, we propose that the youngest ages at any given elevation likely represent the closest-limiting deglacial exposure age and use those ages for our reconstructed ice thinning histories.

Due to differing proportions of spallation versus epithermal and thermal neutron production of ^{36}Cl in each sample, erosion and pore water content can result in nonuniform effects on surface exposure ages (Gosse & Phillips, 2001). The apparent exposure age of samples dominated by production through neutron capture might increase due to erosive processes, whereas erosion will decrease in apparent age of samples with spallation-dominant production. The effects of erosion were tested using a conservative estimate of erosion (1 mm/ka; Ballantyne & Stone, 2012) and result in all but four ages falling within 1-sigma analytical uncertainty of those reported, and the remaining four falling within 1-sigma of the full uncertainty (Table S1).

5. Discussion

5.1. Thinning Timing and Rates

Geologic constraints on former surface elevations of the LIS in the northeastern United States exist as exposure ages of mountain summits (>1,300 m asl; Bierman et al., 2015; Davis et al., 2015; Figure 1), an inland vertical transect (1,200 to ~400 m asl; Corbett et al., 2019), and a coastal, low-elevation vertical transect (≤460 m asl; Koester et al., 2017). Paired ^{10}Be-^{26}Al ages from Mount Washington, New Hampshire (1,896 m asl) and Mount Katahdin, Maine (1,607 m asl) range from 140.1 ± 1.9 to 9.8 ± 0.2 ka and reflect influences of geologic uncertainty including nuclide inheritance from nonerosive cold-based ice coverage, erosion of sampled surfaces, or exhumation from till cover (Bierman et al., 2015). The ^{10}Be ages from Acadia National Park in coastal Maine (≤460 m asl)

Table 1
Average Ice Sheet Thinning Rate Calculations

	Adirondacks ^{36}Cl minimum[a]	Adirondacks ^{36}Cl maximum[b]	G12[c]
Early thinning interval			
Start of interval (t_1) (ka)	21.6	18.2	20.0
End of interval (t_2) (ka)	13.8	17.2	15.5
Δt (kyr)	7.8	1	4.5
Elevation at t_1 (m)	1560	1560	1530
Elevation at t_2 (m)	1387	1387	1217
Δelevation (m)	173	173	313
Average thinning rate (m/year)	0.02	0.17	0.07
Late thinning interval			
Start of interval (t_3) (ka)	17.2	13.8	15.5
End of interval (t_4) (ka)	13.0	15.6	13.5
Δt (kyr)	4.2	*−1.8*[d]	2.0
Elevation at t_3 (m)	1387	1387	1217
Elevation at t_4 (m)	403	403	0
Δelevation (m)	984	984	1217
Average thinning rate (m/kyr)	0.23	*≥0.98*	0.61

[a]Determined by the largest distance between ^{36}Cl ages and their 1-sigma uncertainty. [b]Determined by the smallest distance between ^{36}Cl ages and their 1-sigma uncertainty. [c]Gregoire et al. (2012). [d]Considered as zero for the thinning rate calculation with the resulting thinning rate presented as a minimum limiting rates.

demonstrate rapid ice sheet thinning 15.4 ± 0.4 ka (Figure 1; Koester et al., 2017). Similarly, ^{10}Be and in situ ^{14}C ages from Mount Mansfield in Vermont suggest rapid thinning of the LIS between 1,200 and ~400 m asl ~13.9 ± 0.6 ka (Corbett et al., 2019). Together, these data indicate dynamic differences in the LIS, with high-elevation sites experiencing cold-based ice coverage and low-elevation sites experiencing rapid thinning of erosive, warm-based ice. Thus, our data from the Adirondacks fill both a chronologic and vertical hole in the present data coverage and provide new insights on LIS thinning and retreat in the region.

Ice-scoured bedrock features on the high peaks and bedrock benches of the Adirondacks indicate that erosive warm-based ice likely existed from 400 to 1,560 m asl during the last glacial cycle. With the exception of two ^{36}Cl ages from >1,260 m asl (77.7 ± 1.2, 43.1 ± 1.5 ka), all surface exposure ages from this study postdate the local LGM (~27 ka; Balco et al., 2002; Corbett et al., 2017). In contrast, the summit bedrock samples in New Hampshire and Maine from Bierman et al. (2015) exhibit a wider range of exposure ages with varying degrees of nuclide inheritance and indicate cold-based ice conditions at those locations. Coherency within our sample populations implies little to no inheritance from prior exposure in our data (Figure 3a). Thus, we interpret these ages to reflect the timing of glacial thinning in the region.

If we consider the youngest dates from each site to represent the closest-limiting age of ice retreat, the high-elevation ages indicate that the LIS thinned by 170 m between 19.9 ± 0.5 ka (ADK-AQ-02-15; 1,560 m asl) and 15.5 ± 0.4 ka (ADK-G-02-15; 1,387 m asl; Figure 3a). Taking into account full age uncertainty, average thinning rates for this time interval yield maximum and minimum rates of ~0.17 and ~0.02 m/year, respectively (Table 1). This relatively slow rate of thinning was followed by a period of rapid ice surface lowering from ~1,390 to ~400 m asl between 15.5 ± 0.4 and 14.3 ± 0.4 ka. Maximum and minimum thinning rates for the later interval are ≥0.98 and ~0.23 m/year, respectively (Table 1) with the maximum value similar to Holocene rates of thinning reconstructed for Pine Island Glacier in Antarctica (Johnson et al., 2014). We consider these changes as representing two separate periods of LIS thinning in the Adirondacks.

Previously published ice-thickness histories of the southeastern LIS determined from dynamic ice sheet modeling driven by imposed climate forcings suggest thinning of ~300 m over the Adirondacks from 20.0 to 15.5 ka, with an average thinning rate of ~70 m/ka (Figure 3d; Gregoire et al., 2012). This model result falls within the range of thinning rates suggested by our exposure ages (Figure 3d). Subsequent modeled ice thinning of 1,220 m over the Adirondacks is simulated to have occurred between 15.5 and 13.5 ka at an average rate of ~610 m/kyr, which also falls within the range of our inferred thinning rates during this same interval (Figure 3d). This data-model agreement supports a two-phase thinning history of gradual, early-phase thinning initiated 19.9 ± 0.5 ka, and rapid thinning in the latter phase between 15.5 ± 0.4 and 14.3 ± 0.4 ka (Figure 3d).

5.2. Regional Context

Initial retreat of the LIS from its LGM margins on Martha's Vineyard and Long Island began 27.3 ± 2.2 ka (Balco et al., 2002). Subsequent LIS retreat is documented by recessional moraines in coastal Connecticut, which are dated to 20.7 ± 0.7 ka (Balco & Schaefer, 2006). The early deglacial thinning recorded in our data at ~20 ka indicates that initial exposure of the Adirondack peaks was broadly coincident with lateral retreat of the LIS from its recessional margins in Connecticut. The lack of prominent moraine belts between coastal Connecticut and the ~14 ka Littleton-Bethlehem moraine north of the White Mountains in New Hampshire implies steady retreat of the LIS in this region (Figure 1; Bromley et al., 2015; Thompson et al., 2017).

The North American Varve Chronology provides further evidence for the retreat history of the southeastern sector of the LIS during the deglacial period (Ridge et al., 2012). These records reveal that the Connecticut and Hudson River Valleys also experienced a two-phase pattern of deglaciation, with steady retreat starting ~20 ka until it increased at 14.5 ka, coincident with onset of the Bølling-Allerød warm interval (14.6 ka; Figures 3b and 3c; Rasmussen et al., 2008). Therefore, the period of rapid thinning ~14 ka recorded in the Adirondacks may mirror this increased rate of margin retreat and be a response to Bølling-Allerød warming. Such a regionally consistent pattern may suggest that this region was an important contributor to Meltwater Pulse 1a—a period of rapid sea level rise at this time (Carlson & Clark, 2012). A data-model assessment of sea level contributions to Meltwater Pulse 1a provides a broad range of estimates for Northern and Southern Hemisphere sources, and suggests a 2.8–9.0-m eustatic sea level contribution from North American ice sheets (Liu et al., 2016). Our data provide further geologic constraints on the size of the southeast sector of the LIS, allowing for improved accuracy of sea level contribution estimates during the last deglaciation.

The Mohawk River Valley, located ~100 km south of our field sites, acted as a conduit for meltwater and proglacial lake drainage to the Hudson River Valley while the LIS occupied the Adirondacks. The ^{10}Be ages from strath terraces in the Mohawk River Valley suggest that meltwater flooding through that routing pathway concluded by 14.8 ± 1.3 ka (Porreca et al., 2018) coincident within uncertainty with the abrupt thinning of the LIS recorded by our late deglacial ages. Once the LIS retreated north of the Adirondacks as indicated by our youngest ages, meltwater was rerouted north through the newly exposed Covey Hill col and down the Lake Champlain and the Hudson River Valley (Figure 1; Pair & Rodrigues, 1993; Rayburn et al., 2005; Franzi et al., 2016). Associated flood events have been suggested as a mechanism for meltwater-forced perturbations in thermohaline circulation and the ~400-year Intra-Allerød Cold Period (13.4 ka; Donnelly et al., 2005).

6. Conclusions

New ^{36}Cl exposure ages from boulders and bedrock along vertical transects in the Adirondack Mountains of New York provide insight into the thinning history of the LIS in this region. Our data indicate that the Adirondack peaks were initially exposed ~20 ka and the LIS thinned at a relatively slow rate for several thousands of years, until thinning accelerated from 15.4 ± 1.0 to 13.9 ± 0.9 ka. Ice sheet model simulations reproduce this two-phase pattern of regional LIS thinning during the last deglaciation (Gregoire et al., 2012). Our geologic data reinforce these modeling simulations in suggesting a period of rapid ice loss broadly correlative with the Bølling-Allerød warming and meltwater routing histories (Clark et al., 2001), and imply that some portion of the southeastern LIS may have contributed to the abrupt Meltwater Pulse-1a sea level event 14.6 ka (Carlson & Clark, 2012).

Acknowledgments
We thank Alexander Horvath and Alexandria Koester for the assistance with fieldwork; Andrew Wickert for providing the ice sheet model output; Paul Bierman and Lee Corbett for the helpful discussions; and Joanne Johnson, Mike Bentley, and one anonymous reviewer for their helpful comments that greatly improved this paper. Marcott acknowledges financial support from the University of Wisconsin-Madison. All data from this research are available in the supporting information. We thank Susan Zimmerman, Alan Hidy, and Bob Finkel for their careful AMS measurements and help with interpreting the data. The data sets cited in this paper are available through PANGAEA: Chlorine-36 concentration data for surface exposure age calculations from the Adirondacks (https://doi.pangaea.de/10.1594/PANGAEA.900839).

References

Applegate, P. J., Urban, N. M., Laabs, B. J. C., Keller, K., & Alley, R. B. (2010). Modeling the statistical distributions of cosmogenic exposure dates from moraines. *Geoscientific Model Development*, *3*(1), 293–307. https://doi.org/10.5194/gmd-3-293-2010

Ashwal, L. D. (1993). *Anorthosites* (p. 422). New York: Springer-Berlag. https://doi.org/10.1007/978-3-642-77440-9

Balco, G., Briner, J., Finkel, R. C., Rayburn, J. A., Ridge, J. C., & Schaefer, J. M. (2009). Regional beryllium-10 production rate calibration for late-glacial northeastern North America. *Quaternary Geochronology*, *4*(2), 93–107. https://doi.org/10.1016/j.quageo.2008.09.001

Balco, G., & Schaefer, J. (2006). Cosmogenic-nuclide and varve chronologies for the deglaciation of southern New England. *Quaternary Geochronology*, *1*(1), 15–28. https://doi.org/10.1016/j.quageo.2006.06.014

Balco, G., Stone, J. O., Lifton, N. A., & Dunai, T. J. (2008). A complete and easily accessible means of calculating surface exposure ages or erosion rates from ^{10}Be and ^{26}Al measurements. *Quaternary Geochronology*, *3*(3), 174–195. https://doi.org/10.1016/j.quageo.2007.12.001

Balco, G., Stone, J. O., Porter, S., & Caffee, M. (2002). Cosmogenic nuclide ages for New England coastal moraines, Martha's Vineyard and Cape Cod, Massachusetts, USA. *Quaternary Science Reviews*, *21*(20-22), 2127–2135. https://doi.org/10.1016/S0277-3791(02)00085-9

Ballantyne, C. K., & Stone, J. O. (2012). Did large ice caps persist on low ground in north-west Scotland during the Lateglacial Interstade? *Journal of Quaternary Science*, *27*(3), 297–306. https://doi.org/10.1002/jqs.1544

Bierman, P. R., Davis, P. T., Corbett, L. B., Lifton, N. A., & Finkel, R. C. (2015). Cold-based Laurentide ice covered New England's highest summits during the Last Glacial Maximum. *Geology*, *43*, 1059–1062.

Braconnot, P., Harrison, S. P., Kageyama, M., Bartlein, P. J., Masson-Delmotte, V., Abe-Ouchi, A., et al. (2012). Evaluation of climate models using palaeoclimatic data. *Nature Climate Change*, *2*(6), 417–424. https://doi.org/10.1038/nclimate1456

Bromley, G. R., Hall, B. L., Thompson, W. B., Kaplan, M. R., Garcia, J. L., & Schaefer, J. M. (2015). Later glacial fluctuations of the Laurentide Ice Sheet in the White Mountains of Maine and New Hampshire, U.S.A. *Quaternary Research*, *83*(3), 522–530. https://doi.org/10.1016/j.yqres.2015.02.004

Carlson, A. E., & Clark, P. U. (2012). Ice sheet sources of sea level rise and freshwater discharge during the last deglaciation. *Reviews of Geophysics*, *50*, RG4007. https://doi.org/10.1029/2011RG000371

Clark, P. U., Dyke, A. S., Shakun, J. D., Carlson, A. E., Clark, J., Wohlfarth, B., et al. (2009). The Last Glacial Maximum. *Science*, *325*(5941), 710–714. https://doi.org/10.1126/science.1172873

Clark, P. U., Marshall, S. J., Clarke, G. K. C., Hostetler, S. W., Licciardi, J. M., & Teller, J. T. (2001). Freshwater forcing of abrupt climate change during the Last Deglaciation. *Science*, *293*(5528), 283–287. https://doi.org/10.1126/science.1062517

Clark, P. U., & Mix, A. C. (2002). Ice sheets and sea level of the Last Glacial Maximum. *Quaternary Science Reviews*, *21*(1-3), 1–7. https://doi.org/10.1016/S0277-3791(01)00118-4

Corbett, L. B., Bierman, P. R., Stone, B. D., Caffee, M. W., & Larsen, P. L. (2017). Cosmogenic nuclude age estimate for Laurentide Ice Sheet recession from the terminal moraine, New Jersey, USA, and constraints on the latest Pleistocene ice sheet history. *Quaternary Research*, *87*(3), 482–498. https://doi.org/10.1017/qua.2017.11

Corbett, L. B., Bierman, P. R., Wright, S. F., Shakun, J. D., Davis, P. T., Goehring, B. M., et al. (2019). Analysis of multiple cosmogenic nuclides constrain Laurentide Ice Sheet history and process on Mt. Mansfield, Vermont's highest peak. *Quaternary Science Reviews*, *205*, 234–246. https://doi.org/10.1016/j.quascirev.2018.12.014

Davis, P. T., Bierman, P. R., Corbett, L. B., & Finkel, R. C. (2015). Cosmogenic exposure age evidence for rapid Laurentide deglaciation of the Katahdin area, west-central Maine, USA, 16 to 15 ka. *Quaternary Science Reviews*, *116*, 95–105. https://doi.org/10.1016/j.quascirev.2015.03.021

Denny, C. S. (1974). *Pleistocene geology of the Northeast Adirondack region*. New York: U.S. Department of the Interior.

Donnelly, J. P., Driscoll, N. W., Uchupi, E., Keigwin, L. D., Schwab, W. C., Thieler, E. R., & Swift, S. A. (2005). Catastrophic meltwater discharge down the Husdon Valley: A potential trigger for the Intra-Allerød cold period. *Geology*, *33*(2), 89–92. https://doi.org/10.1130/G21043.1

Dyke, A. S. (2004). An outline of North American Deglaciation with emphasis on central and northern Canada. *Developments in Quaternary Sciences*, *2*, 373–424. https://doi.org/10.1016/S1571-0866(04)80209-4

Faure, G. (1986). *Principles of isotope geology* (p. 589). New York: Wiley.

Franzi, D. A., Ridge, J. C., Pair, D. L., DeSimone, D., Rayburn, J. A., & Barclay, D. J. (2016). Post-Valley Heads deglaciation of the Adirondack Mountains and adjacent lowlands. *Adirondack Journal of Environmental Studies*, *21*, 119–146.

Gosse, J. C., & Phillips, F. M. (2001). Terrestrial in situ cosmogenic nuclides: theory and application. *Quaternary Science Reviews*, *20*(14), 1475–1560. https://doi.org/10.1016/S0277-3791(00)00171-2

Gregoire, L. J., Payne, A. J., & Valdes, P. J. (2012). Deglacial rapid sea level rises caused by ice-sheet saddle collapes. *Nature*, *487*(7406), 219–222. https://doi.org/10.1038/nature11257

Heyman, J., Stroeven, A. P., Harbor, J., & Caffee, M. W. (2011). Too young or too old: evaluating cosmogenic exposure dating based on the analysis of compiled boulder exposure ages. *Earth and Planetary Science Letters*, *302*(1-2), 71–80. https://doi.org/10.1016/j.epsl.2010.11.040

Hostetler, S. W., Bartlein, P. J., Clark, P. U., Small, E. E., & Soloman, A. M. (2000). Simulated influences of Lake Agassiz on the climate of central North America 11,000 years ago. *Nature*, *405*(6784), 334–337. https://doi.org/10.1038/35012581

Isachsen, Y. W., & Fisher, D. W. (1970). *Geologic map of New York State, Adirondack Sheet* (Vol. 16). Albany, NY: State Science Service Map and Chart Series.

Johnson, J. S., Bentley, M. J., Smith, J. A., Finkel, R. C., Rood, D. H., Gohl, K., et al. (2014). Rapid thinning of Pine Island Glacier in the Early Holocene. *Science*, *343*(6174), 999–1001. https://doi.org/10.1126/science.1247385

Kemp, J. F. (1898). *Geology of the Lake Placid region* (Vol. 5, pp. 51–67). Albany, NY: State Museum Bulletin.

Kemp, J. F. (1920). *Geology of the Mount Marcy quadrangle* (Vol. 229, p. 137). Albany, NY: N.Y. State Museum Bulletin.

Koester, A. J., Shakun, J. D., Bierman, P. R., Davis, P. T., Corbett, L. B., Braun, D., & Zimmerman, S. R. (2017). Rapid thinning of the Laurentide Ice Sheet in coastal Maine, USA, during late Heinrich Stadial 1. *Quaternary Science Reviews*, *163*, 180–192. https://doi.org/10.1016/j.quascirev.2017.03.005

Lambeck, K., Rouby, H., Purcell, A., Sun, Y., & Sambridge, M. (2014). Sea level and global ice volumes from the Last Glacial Maximum to the Holocene. *Proceedings of the National Academy of Sciences of the United States of America*, *111*(43), 15,296–15,303. https://doi.org/10.1073/pnas.1411762111

Licciardi, J. M., Denoncourt, C. L., & Finkel, R. C. (2008). Cosmogenic ^{36}Cl production rates from Ca spallation in Iceland. *Earth and Planetary Science Letters*, *267*(1-2), 365–377. https://doi.org/10.1016/j.epsl.2007.11.036

Lifton, N., Sato, T., & Dunai, T. J. (2014). Scaling in situ cosmogenic nuclide production rates using analytical approximations to atmospheric cosmic-ray fluxes. *Earth and Planetary Science Letters*, *386*, 149–160. https://doi.org/10.1016/j.epsl.2013.10.052

Liu, J., Milne, G. A., Kopp, R. E., Clark, P. U., & Shennan, I. (2016). Sea-level constraints on the amplitude and source distribution of Meltwater Pulse 1A. *Nature Geoscience*, *9*(2), 130–134. https://doi.org/10.1038/ngeo2616

Marrero, S. M., Phillips, F. M., Borchers, B., Lifton, N., Aumer, R., & Balco, G. (2016). Cosmogenic nuclide systematics and the CRONUScalc program. *Quaternary Geochronology*, *31*, 160–187. https://doi.org/10.1016/j.quageo.2015.09.005

Ogilvie, I. H. (1902). Glacial phenomena in the Adirondacks and Champlain Valley. *The Journal of Geology*, *10*(4), 397–412. https://doi.org/10.1086/621013

Pair, D. L., & Rodrigues, C. G. (1993). Late Quaternary deglaciation of the southwestern St. Lawrence Lowland, New York and Ontario. *Geological Society of America Bulletin*, *105*(9), 1151–1164. https://doi.org/10.1130/0016-7606(1993)105<1151:LQDOTS>2.3.CO;2

Peltier, W. R., Argus, D. F., & Drummond, R. (2015). Space geodesy constrains ice age terminal deglaciation: The global ICE-6G_C (VM5a) model. *Journal of Geophysical Research: Solid Earth*, *120*, 450–487. https://doi.org/10.1002/2014JB011176

Porreca, C., Briner, J. P., & Kozlowski, A. (2018). Laurentide ice sheet meltwater routing along the Iro-Mohawk River, eastern New York, USA. *Geomorphology*, *303*, 155–161. https://doi.org/10.1016/j.geomorph.2017.12.001

Putkonen, J., & Swanson, T. (2003). Accuracy of cosmogenic ages for moraines. *Quaternary Research*, *59*(2), 255–261. https://doi.org/10.1016/S0033-5894(03)00006-1

Rasmussen, S. O., Seierstad, I. K., Andersen, K. K., Bigler, M., Dahl-Jensen, D., & Johnsen, S. J. (2008). Synchronization of the NGRIP, GRIP, and GISP2 ice cores across MIS 2 and palaeoclimatic implications. *Quaternary Science Reviews*, *27*(1-2), 18–28. https://doi.org/10.1016/j.quascirev.2007.01.016

Rayburn, J. A., Knuepfer, P. L. K., & Franzi, D. A. (2005). A series of large, Wisconsinan meltwater floods through the Champlain and Hudson Valleys, New York State, USA. *Quaternary Science Reviews*, *24*(22), 2410–2419. https://doi.org/10.1016/j.quascirev.2005.02.010

Ridge, J. C., Balco, G., Bayless, R. L., Beck, C. C., Carter, L. B., Dean, J. L., et al. (2012). The New North American Varve Chronology: A precise record of southeastern Laurentide Ice Sheet deglaciation and climate, 18.2–12.5 kyr BP, and correlations with Greenland ice core records. *American Journal of Science*, *312*(7), 685–722. https://doi.org/10.2475/07.2012.01

Stone, J. O., Fifield, L. K., Allan, G. L., & Cresswell, R. G. (1996). Cosmogenic chlorine-36 from calcium spallation. *Geochimica et Cosmochimica Acta*, *60*(4), 679–692. https://doi.org/10.1016/0016-7037(95)00429-7

Thompson, W. B., Dorion, C. C., Ridge, J. C., Balco, G., Fowler, B. K., & Svendsen, K. M. (2017). Deglaciation and late-glacial climate change in the White Mountains, New Hampshire, USA. *Quaternary Research*, *87*(1), 96–120. https://doi.org/10.1017/qua.2016.4

Zhang, X., Lohmann, G., Knorr, G., & Purcell, C. (2014). Abrupt climate change shifts controlled by ice sheet changes. *Nature*, *512*(7514), 290–294. https://doi.org/10.1038/nature13592